

Large-angle Bhabha scattering and luminosity at flavour factories

C.M. Carloni Calame^a C. Lunardini^b G. Montagna^a
O. Nicrosini^c F. Piccinini^c

^a*Dipartimento di Fisica Nucleare e Teorica, Università di Pavia, and INFN,
Sezione di Pavia, via A.Bassi 6, 27100, Pavia, Italy*

^b*SISSA-ISAS, via Beirut 2-4, 34100, Trieste, Italy and INFN, Sezione di Trieste,
via Valerio 2, 34127, Trieste, Italy*

^c*INFN, Sezione di Pavia, and Dipartimento di Fisica Nucleare e Teorica,
Università di Pavia, via A. Bassi 6, 27100, Pavia, Italy*

Abstract

The luminosity determination of electron-positron colliders operating in the region of low-lying hadronic resonances ($E_{cm} \simeq 1-10$ GeV), such as BEPC/BES, DAΦNE, KEKB, PEP-II and VEPP-2M, requires the precision calculation of the Bhabha process at large scattering angles. In order to achieve a theoretical accuracy at a few 0.1% level, the inclusion of radiative corrections is mandatory. The phenomenologically relevant effect of QED corrections is taken into account in the framework of the Parton Shower (PS) method, which is employed both for cross section calculation and event generation. To test the reliability of the approach, a benchmark calculation, including exact $O(\alpha)$ corrections and higher-order leading logarithmic contributions, is developed as well and compared in detail with the PS predictions. The effect of $O(\alpha)$ next-to-leading and higher-order leading corrections is investigated in the presence of realistic event selections for the Bhabha process at the Φ factories. A new Monte Carlo generator for data analysis (BABAYAGA) is presented, with an estimated accuracy of 0.5%. Possible developments aiming at improving its precision and range of applicability are discussed.

Key words: electron-positron collision, flavour factories, Bhabha scattering, radiative corrections, Parton Shower, Monte Carlo.

PACS: 02.70.Lq,12.20.Ds,13.10.+q

1 Introduction

The accurate determination of the machine luminosity is a fundamental ingredient for the successful accomplishment of the physics programme of electron-positron (e^+e^-) colliders operating in the region of the low-lying hadronic resonances, such as BEPC/BES (Beijing), DAΦNE (Frascati), VEPP-2M (Novosibirsk), as well as for the BELLE and BABAR experiments around the Υ at KEKB (KEK) and PEP-II (SLAC). In particular, the precise measurement of the hadronic cross section at the Φ factories requires a luminosity determination with a total relative error better than 1% [1–4]. As well known, the luminosity L of e^+e^- colliders can be precisely derived via the relation $L = N/\sigma_{th}$, where N and σ_{th} are the number of events and the theoretical cross section of a given reference reaction, respectively. In order to make the total (experimental and theoretical) luminosity error as small as possible, the cross section σ_{th} of the reference process should be large, in order to keep the statistical uncertainty small, and calculable with high theoretical accuracy.

At e^+e^- machines operating in the energy range 1-10 GeV, the best candidate fulfilling the above criteria is the process $e^+e^- \rightarrow e^+e^-$ (Bhabha scattering) detected at large scattering angles, say in the angular range $20^\circ \leq \vartheta \leq 160^\circ$. For example, at the Φ factory DAΦNE the KLOE detector can be used to detect such events [4], where the Bhabha scattering cross section is significant, being of the order of 10^4 nb at a center of mass (c.m.) energy around the Φ resonance ($\sqrt{s} \simeq 1$ GeV).

Therefore, on theoretical side, precision calculations of the large-angle Bhabha (LABH) cross section are demanded, with a theoretical accuracy at a few 0.1% level. This implies to include in the calculation all the phenomenologically relevant radiative corrections, in particular the large effects due to photonic radiation. Furthermore, such effects should be implemented and accurately simulated in event generators, which are strongly demanded by the experimental analysis.

At present, the status of the theoretical predictions and generators of interest for the LABH process at low-energy e^+e^- machines can be summarized as follows. An exact $O(\alpha)$ generator, based on the calculation of ref. [5] and modified to match DAΦNE characteristics, is used in Monte Carlo (MC) studies by the KLOE collaboration [4,6]. An independent $O(\alpha)$ generator is also in use by the CMD-2 and SND experiments at VEPP-2M [7]. In both the programs used in such MC simulations the effect of higher-order corrections is not taken into account. A semi-analytical calculation of the cross section for large-angle QED processes, i.e. $e^+e^- \rightarrow \mu^+\mu^-, e^+e^-, \gamma\gamma$, below 3 GeV was performed in ref. [8]. It includes exact $O(\alpha)$ plus leading logarithmic (LL) higher-order corrections. This formulation is available as a computer code de-

scribed in ref. [9]. The recently developed Bhabha generator BHWIDE [10], based on the Yennie-Frautschi-Suura approach for the treatment of QED radiation, appears in the list of simulation tools presently under consideration by the BABAR collaboration at the B factory PEP-II [11]. A QED Parton Shower (PS) algorithm, which is employed in the present study, is adopted in refs. [12,13] for the computation of radiative corrections to LABH scattering. These calculations, however, are optimized to high-energy LABH and differ, as it will be discussed, in some aspects from the present implementation of the PS model. A complete inventory of existing calculations and programs, for both small- and large-angle Bhabha scattering, used at very high-energy e^+e^- colliders can be found in ref. [14].

The paper is organized as follows. In Sect. 2 the theoretical formulation, which is based upon a QED realization of the PS method to account for radiative corrections due to photon emission, is described. The steps and kinematics of the algorithm are reviewed. Sect. 3 is devoted to the description of a new, original PS generator for the simulation of the LABH process and based upon the formulation previously discussed. A first sample of numerical results from the PS Bhabha generator is also given, with particular emphasis on the simulation of the Bhabha process at the Φ factories in the presence of realistic event selections (ES). In the following Sections tests of the reliability of the PS approach are shown and commented, both at the level of integrated cross sections and differential distributions. To this end, the calculation of the exact $O(\alpha)$ cross section and its matching with higher-order LL corrections is addressed in Sect. 4. This is meant as a benchmark calculation, developed in order to check the physical+technical precision of the PS generator. Detailed comparisons between the PS predictions and the results of the benchmark computation are given in Sect. 5. Conclusions, open issues and possible developments are discussed in Sect. 6.

2 Theoretical approach and the Parton Shower method

In order to approach the aimed theoretical accuracy, the calculation of the QED corrected Bhabha scattering cross section and the relative event generation is performed according to the master formula [15]:

$$\sigma(s) = \int dx_- dx_+ dy_- dy_+ \int d\Omega_{lab} D(x_-, Q^2) D(x_+, Q^2) \times \\ D(y_-, Q^2) D(y_+, Q^2) \frac{d\sigma_0}{d\Omega_{cm}}(x_- x_+ s, \vartheta_{cm}) J(x_-, x_+, \vartheta_{lab}) \Theta(cuts), \quad (1)$$

which is based on the factorization theorems of (universal) infrared and collinear singularities. Equation (1) can be worked out within a QED PS algorithm

for the calculation of the electron Structure Function (SF) $D(x, Q^2)$, both for initial-state radiation (ISR) and final-state radiation (FSR). In eq. (1) $d\sigma_0/d\Omega$ is the Born-like differential cross section relevant for centre c.m. energy between 1-10 GeV, including the photonic s - and t -channel diagrams and their interference, and the contributions due to exchange of vector resonances, such as Φ , J/Ψ and Υ . Following the standard procedure described in ref. [16], the contribution of hadronic resonances is taken into account in terms of their effective couplings to the electron. At c.m. energy around 1 GeV, the total Φ contribution amounts to $\approx 0.1(0.3)\%$ for $20^\circ(50^\circ) \leq \vartheta \leq 160^\circ(130^\circ)$, where ϑ is the electron scattering angle. For higher energies, as in the case of BELLE and BABAR experiments around the Υ , the effect of the Υ resonance to the Bhabha cross section is of the same order. It is worth noticing that for the low-energy colliders the LABH cross section is largely dominated by t -channel photon exchange; hence, its leading dynamics is quite similar to small-angle Bhabha (SABH) at LEP1/SLC and LABH at LEP2 and higher energies [14]. In the hard-scattering cross section, the relevant correction due to vacuum polarization is taken into account as well, by adopting the parameterization of ref. [17]. In the evaluation of the hadronic contribution to the vacuum polarization, the Euclidean value of the momentum in the photon propagator has been used as the appropriate scale for time-like momenta [18]. The effect of the running coupling constant at $\sqrt{s} = M_\Phi$ is to enhance the cross section by $\approx 2(2.5)\%$ for $20^\circ(50^\circ) \leq \vartheta \leq 160^\circ(130^\circ)$. The factor $J(x_-, x_+, \vartheta_{lab})$ in eq. (1) accounts for the boost from the c.m. to the lab frame due to emission of unbalanced ISR from the electron and positron legs, while $\Theta(cuts)$ represents cuts implementation.

The basic ingredient of eq. (1) is the electron SF $D(x, Q^2)$, which represents the probability density of finding “inside” a parent electron an electron with momentum fraction x and virtuality Q^2 . It can be explicitly obtained in QED by solving the Dokshitzer-Gribov-Lipatov-Altarelli-Parisi (DGLAP) evolution equation [19] in the non-singlet channel:

$$Q^2 \frac{\partial}{\partial Q^2} D(x, Q^2) = \frac{\alpha}{2\pi} \int_x^1 \frac{dy}{y} P_+(y) D\left(\frac{x}{y}, Q^2\right), \quad (2)$$

where $P_+(x)$ is the regularized $e \rightarrow e + \gamma$ splitting function

$$P_+(x) = \frac{1+x^2}{1-x} - \delta(1-x) \int_0^1 dt P(t). \quad (3)$$

Notice that the energy scale Q^2 entering the SF will be, in general, dependent on the specific process under study. No *exact* analytical solution of eq. (2) is known in the literature. After the efforts undertaken in the last decade for

the program of precision physics at LEP/SLC, the theoretical situation can be summarized as follows (see for instance ref. [20] and references therein):

- (1) approximate (accurate) analytical solutions in the collinear limit [21]. This kind of SFs is implemented in most of the programs for data analysis at LEP/SLC [20];
- (2) exact numerical solution, obtained via a numerical calculation of the Mellin transform of the SF. This can be considered as a benchmark solution, but it is unusable from the practical point of view for implementation in computational tools;
- (3) exact MC solution, obtained by means of the PS approach, which is particularly powerful for exclusive event generation [22–24]. The PS method, originally developed and widely applied in perturbative QCD [22], has been recently introduced in QED [23,24] as a convenient framework to compute photonic radiative corrections in e^+e^- collisions. In fact, exponentiation of soft photons and the contribution of multiple emission of hard collinear photons can be automatically accounted for.

Let us summarize the basics of the PS method. The starting point of the PS approach is the Sudakov form factor [25]:

$$\Pi(s_1, s_2) = \exp \left[-\frac{\alpha}{2\pi} \int_{s_2}^{s_1} \frac{ds'}{s'} \int_0^{x_+} dz P(z) \right], \quad (4)$$

which represents the probability that an electron evolves from virtuality $-s_2$ to virtuality $-s_1$ with no emission of photons of energy fraction greater than $\epsilon = 1 - x_+$, where ϵ is an infrared regulator. In terms of the factor $\Pi(s_1, s_2)$, the DGLAP equation can be written in iterative form as:

$$\begin{aligned} D(x, s) &= \Pi(s, m^2) \delta(1 - x) \\ &+ \int_{m^2}^s \Pi(s, s') \frac{ds'}{s'} \Pi(s', m^2) \frac{\alpha}{2\pi} \int_0^{x_+} dy P(y) \delta(x - y) \\ &+ \int_{m^2}^s \Pi(s, s') \frac{ds'}{s'} \int_{m^2}^{s'} \Pi(s', s'') \frac{ds''}{s''} \Pi(s'', m^2) \times \\ &\quad \left(\frac{\alpha}{2\pi} \right)^2 \int_0^{x_+} dx_1 \int_0^{x_+} dx_2 P(x_1) P(x_2) \delta(x - x_1 x_2) + \dots \end{aligned} \quad (5)$$

where here $Q^2 = s$ is understood, $s = 4E^2$ being the total c.m. energy. Equation (5) suggests the steps to compute $D(x, s)$ by means of a MC algorithm [22,23]:

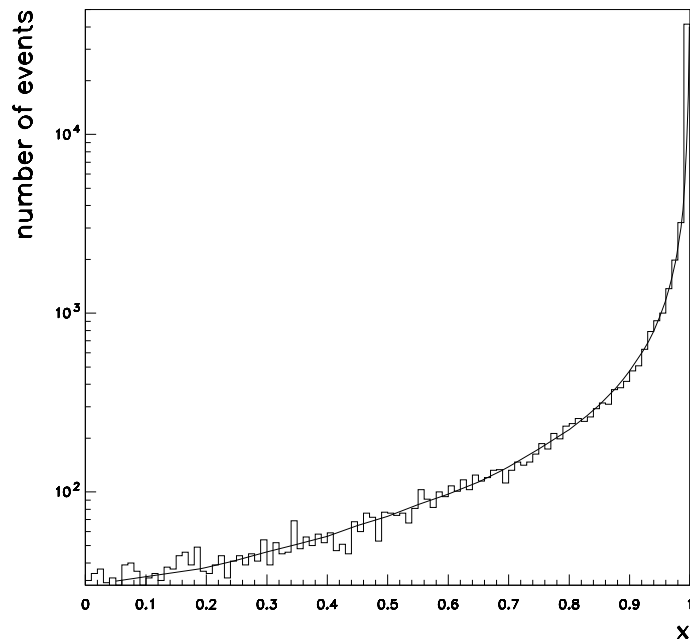


Fig. 1. x distribution of the electron SF at $\sqrt{s} = 190$ GeV. Solid line: numerical solution of DGLAP equation, by means of numerical inversion of Mellin transform. Histogram: result of the PS algorithm.

- (1) Set initial values for the electron virtuality and momentum fraction: $K^2 = m_e^2$ and $x = 1$ (with m_e electron mass).
- (2) Choose a random number ξ in $[0, 1]$.
- (3) If $\xi < \Pi(s, K^2)$ then stop: no photon is radiated.
- (4) Else if $\xi > \Pi(s, K^2)$, a photon is emitted: calculate the value K'^2 of the electron virtuality after the branching as the solution of the equation $\xi = \Pi(K'^2, K^2)$.
- (5) Choose the residual momentum fraction z of the electron in $[0, x_+]$, according to $P(z)$.
- (6) Replace x by zx and K^2 by K'^2 . Go back to step 2.

In this way the emission of a shower of photons by an electron is simulated, and the x distribution of the PS event sample reproduces $D(x, Q^2)$. Such a distribution, obtained from a 10^5 event sample at $Q^2 = s = (190)^2$ GeV², is compared in Fig. 1 with a numerical solution of eq. (2), normalized to the same number of events. The agreement is excellent. A further test of the algorithm is the comparison between the exact analytical Mellin moments $D(N)$ of the SF and the corresponding ones calculated in the PS scheme. This comparison is shown in Fig. 2, where it can be seen that the PS simulation (markers) for $N = 1, 2, 10, 50, 200$ well agrees, within the statistical errors, with the analytical moments (solid line). The results shown in Fig. 1 and Fig. 2 have been obtained with the value $\epsilon = 10^{-9}$ for the infrared cut-off entering eq. (4).

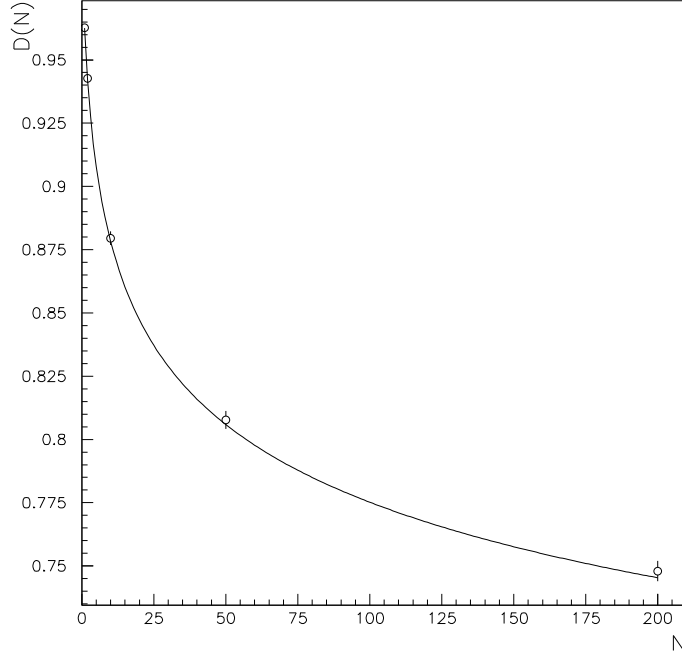


Fig. 2. Comparison for the Mellin moments of the electron SF at $\sqrt{s} = 190$ GeV. Solid line: exact analytical moments. Markers: results of the PS algorithm for $N = 1, 2, 10, 50, 200$.

However, independence of the PS predictions for the QED corrected cross section from ϵ variation, on a wide range of ϵ values (from 10^{-16} to 10^{-4}), has been successfully checked, as shown in Fig. 3 for the LABH cross section at the Φ factory. In the present implementation of the PS model ϵ is taken constant, in order to avoid loss of accuracy in the determination of the absolute value of the electron SF, as first pointed out in ref. [23].

An up to $O(\alpha)$ PS algorithm has been developed as well. It allows to calculate the corrected cross section of eq. (1) up to $O(\alpha)$. Such a calculation is strongly required for fully consistent comparisons between the PS predictions and an exact perturbative calculation. The steps required for the $O(\alpha)$ PS can be obtained by using eq. (5) and expanding the product $D(x_-, Q^2)D(x_+, Q^2)D(y_+, Q^2)D(y_-, Q^2)$ present in eq. (1) up to $O(\alpha)$. It is easy to see that:

$$\begin{aligned}
& [D(x_-, s)D(x_+, s)D(y_+, s)D(y_-, s)]_{O(\alpha)} = \\
& [\Pi^4(s, m^2)]_{O(\alpha)} \delta(1 - x_+) \delta(1 - x_-) \delta(1 - y_+) \delta(1 - y_-) \\
& + \frac{\alpha}{2\pi} \ln \frac{s}{m^2} \{ \delta(1 - x_-) \delta(1 - y_+) \delta(1 - y_-) P(x_+) \\
& \quad + \delta(1 - x_+) \delta(1 - y_+) \delta(1 - y_-) P(x_-)
\end{aligned}$$

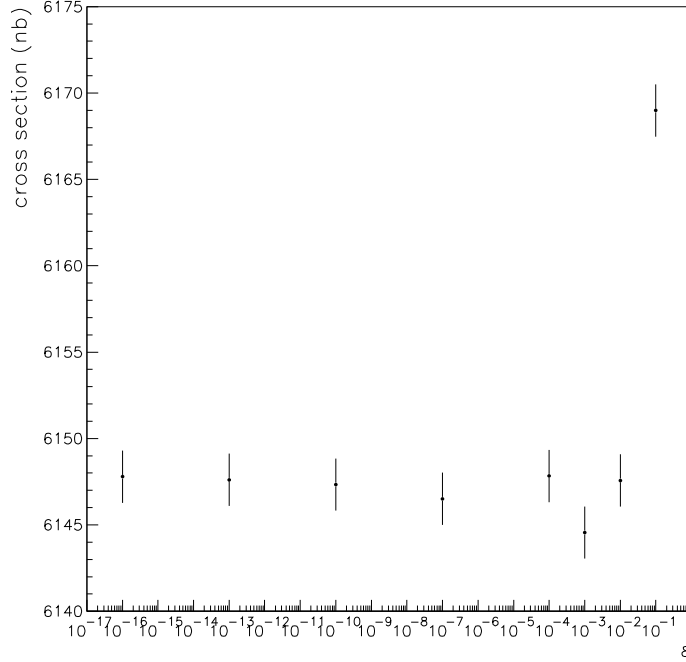


Fig. 3. QED corrected Bhabha cross section as a function of the infrared regulator ϵ , at the peak of the Φ resonance. Cuts used are given in the text and correspond to a realistic event selection at DAΦNE.

$$\begin{aligned}
& +\delta(1-x_+)\delta(1-x_-)\delta(1-y_+)P(y_-) \\
& +\delta(1-x_+)\delta(1-x_-)\delta(1-y_-)P(y_+) \},
\end{aligned} \tag{6}$$

where $[\Pi^4(s, m^2)]_{O(\alpha)}$ is the product of four Sudakov form factors expanded up to $O(\alpha)$.

The steps for $O(\alpha)$ PS are therefore the following:

- (1) Set initial values for the fermions virtuality and momentum fractions: $K^2 = m_e^2$ and $x_+ = x_- = y_+ = y_- = 1$.
- (2) Choose a random number ξ in $[0, 1]$.
- (3) If $\xi < [\Pi^4(s, K^2)]_{O(\alpha)}$ then stop: no photon is radiated.
- (4) Else if $\xi > [\Pi^4(s, K^2)]_{O(\alpha)}$, a photon is emitted: calculate the value K'^2 of the fermion virtuality after the branching as the solution of the equation $\xi = [\Pi^4(K'^2, m^2)]_{O(\alpha)}$.
- (5) Choose randomly the fermion which has emitted the photon.
- (6) Choose the residual momentum fraction z of the fermion in $[0, 1 - \epsilon]$, according to $P(z)$ and replace x_+, x_-, y_+ or y_- with z , according to the particle which has radiated.
- (7) Stop the algorithm.

The PS algorithm, both in the all order and $O(\alpha)$ implementation, offers

the possibility to go naturally beyond the strictly collinear treatment of the electron evolution, by generating the transverse momentum p_{\perp} of electrons and photons at each branching. To this end, a definite role for the variable x must be chosen. In the QED PS model of ref. [23] x is understood as the longitudinal momentum fraction of the electron after photon emission. In the present PS simulation, x is chosen as the energy fraction of the electron after photon emission (hereafter denoted as E scheme), in agreement with the known perturbative results for the photon spectrum in QED [26] and previous interpretation in perturbative QCD (as, for example, in the paper by Marchesini-Webber in ref. [22]). It is worth noticing that the two prescriptions are coincident in the collinear limit. In the E scheme, the kinematics of the branching process $e(p) \rightarrow e'(p') + \gamma(q)$ can be written as:

$$\begin{aligned} p &= (E, \vec{0}, p_z) \\ p' &= (zE, \vec{p}_{\perp}, p'_z) \\ q &= ((1-z)E, -\vec{p}_{\perp}, q_z), \end{aligned} \tag{7}$$

with built-in energy and transverse momentum conservation. After having generated the variables k^2 , k'^2 and z by the PS algorithm, the on-shell conditions $p^2 = k^2$, $p'^2 = k'^2$, $q^2 = 0$, together with the longitudinal momentum conservation, allow to obtain complete event reconstruction as follows:

$$\begin{aligned} p_z &= E - \frac{k^2}{2E} \\ p'_z &= zE - \frac{(1-z)k^2 + k'^2}{2E} \\ q_z &= (1-z)E - \frac{zk^2 - k'^2}{2E} \\ p_{\perp}^2 &= (1-z)(zk^2 - k'^2), \end{aligned} \tag{8}$$

at first order in $k^2/E^2 \ll 1$, $p_{\perp}^2/E^2 \ll 1$. An alternative procedure, followed in the literature [24], consists in generating a photon p_{\perp} according to the leading pole behaviour $1/p \cdot q$. As a cross-check of the results obtained by means of eq. (8), the method of ref. [24] has been also employed in the present implementation of the PS model, finding agreement between the procedures for the calculation of the QED corrected Bhabha cross section.

3 Bhabha generator and first sample of phenomenological results

In the spirit of the PS approach described above, a new MC event generator (BABAYAGA) for simulation of the LABH process at e^+e^- flavour factories

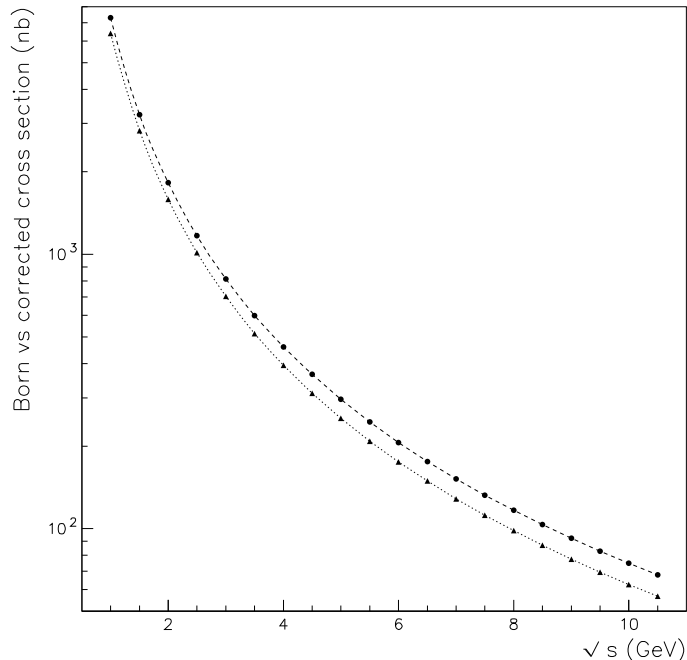


Fig. 4. Comparison between the QED corrected LABH cross section and the Born one, in the c.m. energy range from 1 GeV to 10.5 GeV. Solid circles: Born approximation; solid triangles: QED corrected cross section. Cuts are given in the text.

has been developed. It is a generator of unweighted events, giving as output the QED corrected cross section and the momenta of the final-state particles. Both ISR and FSR are simulated. In principle, an “arbitrary” number of photons can be generated, including their p_{\perp} . In the standard version, BABAYAGA records the momenta of electron and positron, and of the most energetic and next-to-most energetic photons generated by the electromagnetic shower. The possibility of an up to $O(\alpha)$ calculation of eq. (1) is included as an option, in order to compare it with the exact $O(\alpha)$ perturbative results (see Sect. 5). Also for the $O(\alpha)$ branch, particles momenta are reconstructed.

As a first example, in Fig. 4, the PS corrected LABH cross section is compared with the Born-like cross section, as a function of the c.m. energy. An energy threshold of $0.8 \cdot E_{beam}$ for both electron and positron is required, the acceptance cuts are $20^{\circ} \leq \vartheta_{\pm} \leq 160^{\circ}$ and an acollinearity cut of 5° is imposed. In such a situation, the correction due to QED radiation is of the order of 10% at the Φ factories and of the order of 20% at the B factories, pointing out the need of a careful treatment of photonic corrections in simulation tools of the LABH process at flavour factories.

A further sample of phenomenological results obtained by means of the BABAYAGA program is shown in Figs. 5-7. The parameters and selection criteria adopted in the analysis are very similar to those considered in previous

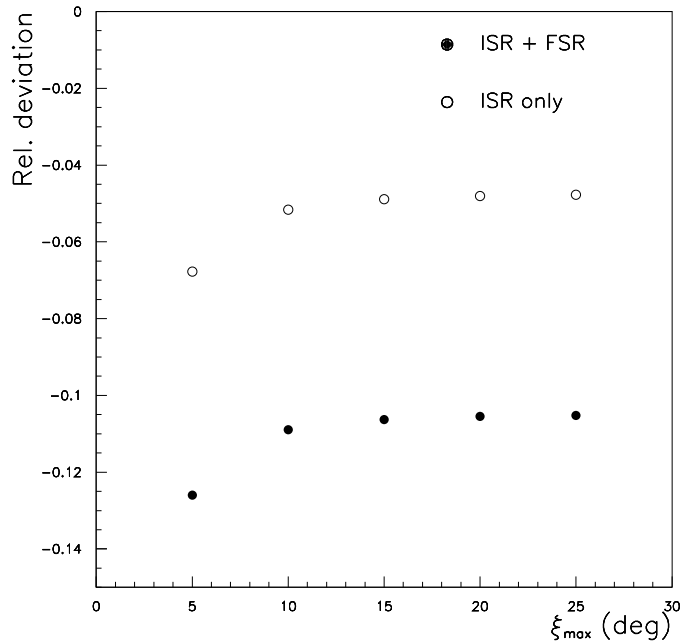


Fig. 5. Relative effect of ISR and ISR+FSR on the integrated Bhabha cross section at the Φ factories. Open circles: ISR only; solid circles: ISR+FSR. Cuts used are given in the text.

MC simulations [4,6] and correspond to realistic data taking at DAΦNE and VEPP-2M, for c.m. energy at the Φ peak, i.e. $\sqrt{s} = 1.019$ GeV. The energy cut imposed on the final-state electron and positron is $E_{min}^{\pm} = 0.4$ GeV; two different angular acceptances of $20^{\circ} \leq \vartheta_{\pm} \leq 160^{\circ}$ and $50^{\circ} \leq \vartheta_{\pm} \leq 130^{\circ}$ are considered, with (maximum) acollinearity cut allowed to vary in the range $\xi_{max} = 5^{\circ}, 10^{\circ}, 15^{\circ}, 20^{\circ}, 25^{\circ}$. The energy cut refers to the energy of the bare electron and positron, corresponding to a so-called bare ES (see for instance ref. [14]), which is not far from realistic due to the presence of magnetic fields as for DAΦNE and CMD-2 experiment at VEPP-2M. The tight acollinearity cut $\xi_{max} = 5^{\circ}$ is generally introduced in MC simulations in order to single out quasi-elastic Bhabha events [4]. However, it is worth noticing that this acollinearity cut, in association with the high energy thresholds on bare electrons and positrons, defines a rather severe set of constraints, which can be expected to emphasize the effects of QED radiative corrections, especially from the final-state. This conjecture is confirmed by the numerical results of Fig. 5, where the (relative) effect, with respect to the Born cross section, of ISR only (open circles) is compared with the whole effect of ISR and FSR (solid circles). Actually, it can be seen that the photon radiation produces a lowering of the integrated cross section of the order of 10% and that half of this effect has to be ascribed to FSR, showing the need of including FSR for realistic simulations. In this simulation, the Q^2 entering the electron SF is fixed to be $Q^2 = s$ as typical virtuality in initial- and final-state shower. The relevance of

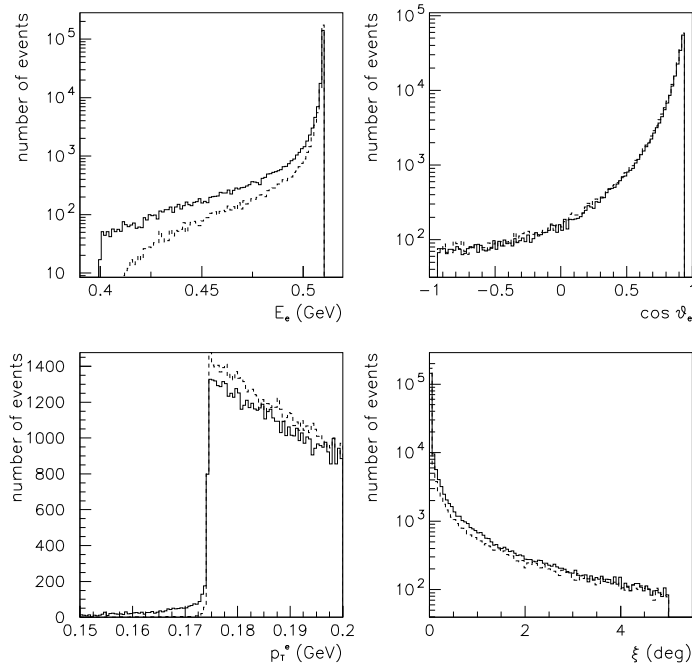


Fig. 6. Effect of FSR on Bhabha differential distributions at the Φ factories: electron energy, electron scattering angle, electron transverse momentum and acollinearity. Dashed histograms: ISR only. Solid histograms: ISR+FSR. Cuts are given in the text.

FSR in such ES is further illustrated in Fig. 6 for the electron energy, electron scattering angle, electron transverse momentum distribution and acollinearity distribution as well. It can be noticed that the electron energy and p_{\perp} are significantly affected by FSR, while this is not the case for the electron scattering angle and acollinearity, which are actually largely dominated, as expected, by the x distribution of ISR [15]. In the comparison shown in Fig. 6 the numbers of generated events for ISR only and ISR+FSR are consistently normalized to the same luminosity.

A further illustration of the potential of BABAYAGA in event generation is given in Fig. 7, showing the energy, polar angle and transverse momentum of the most energetic photon, as well as the missing mass distribution of the event, defined as $\sqrt{(p_+ + p_- - q_+ - q_- - k)^2}$, where $p_{\pm}(q_{\pm})$ are the initial(final) electron/positron momenta and k is the momentum of the most energetic photon. A minimum energy cut of 5 MeV is imposed as visibility criterion. It can be seen that the expected physical features of photon radiation are correctly reproduced by the PS generator, noticeably the soft peaking behaviour of E_{γ} , p_{\perp}^{γ} and missing mass distribution as well as the initial- and the final-state collinear peaks, which are clearly visible in the $\cos \vartheta_{\gamma}$ distribution.

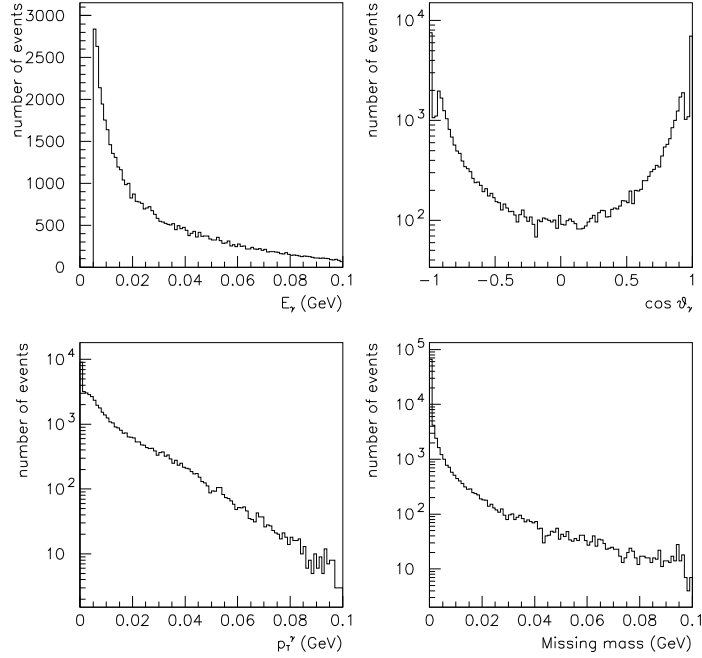


Fig. 7. Distributions of the most-energetic photon in the LABH process at the Φ factories: energy, polar angle, transverse momentum and missing mass. Cuts are given in the text.

4 Benchmark calculation

In order to test the (physical+technical) precision of the PS approach and corresponding Bhabha generator, an *exact* $O(\alpha)$ perturbative calculation has been addressed, by computing the up to $O(\alpha)$ corrected cross section as follows

$$\sigma_{exact}^{(\alpha)} = \sigma_{S+V}^{(\alpha)}(E_\gamma < k_0) + \sigma_H^{(\alpha)}(E_\gamma > k_0, cuts). \quad (9)$$

In the above equation the $O(\alpha)$ soft+virtual part $\sigma_{S+V}^{(\alpha)}$ is obtained by integration over the electron angle of the soft+virtual differential cross section, which is explicitly given by [27]

$$d\sigma_{S+V}^{(\alpha),i} = d\sigma_0 \left\{ 1 + 2 (\beta_e + \beta_{int}) \ln k_0/E + C_F^i \right\}. \quad (10)$$

In eqs. (9) and (10), k_0 stands for a (small) photon energy soft-hard (fictitious) separator, i is an index for the photonic contributions to the Bhabha Born matrix element ($i = |\gamma(s)|^2, |\gamma(t)|^2, \gamma(s)-\gamma(t)$), $\beta_e = 2\alpha/\pi (\ln(s/m_e^2) - 1)$ is the leading collinear factor for initial- and final-state radiation, $\beta_{int} = 2\alpha/\pi \ln(t/u)$ is the leading angular factor for initial-final state interference. Furthermore, in

eq. (10) $C_F^i = C_F^i(\vartheta)$ are the soft+virtual K -factors for the three QED channels, including box/interference finite terms [27]. The hard bremsstrahlung contribution $\sigma_H^{(\alpha)}$ is included, in the photon phase-space region above the energy cut k_0 , via the $e^+e^- \rightarrow e^+e^-\gamma$ matrix element calculated in ref. [28]. Its contribution is computed numerically in the presence of experimental cuts by means of the MC method with standard importance sampling technique, in order to handle collinear and infrared photon singularities. Needless to say, the independence of eq. (9) from the fictitious infrared cut-off k_0 was successfully checked with high numerical precision.

The comparison between the exact $O(\alpha)$ calculation and the $O(\alpha)$ predictions of the PS generator is of interest because it allows to evaluate the size of the $O(\alpha)$ next-to-leading order (NLO) corrections, which are missing in the PS. Moreover, this comparison can be a useful guideline to improve the agreement between perturbative and LL PS results, for example, by properly choosing the virtuality Q^2 in the electron SF in such a way that $O(\alpha)$ NLO terms are effectively reabsorbed into the LL contributions. It can be noticed, in fact, that by choosing the scale Q^2 as $Q^2 = st/u$ in the collinear logs $\ln(Q^2/m^2)$ generated by the PS method, then one has that $\ln(Q^2/m^2) \rightarrow \ln(s/m^2) + \ln(t/u)$ [29]. If this procedure is applied both to ISR and FSR by choosing as maximum virtuality of the electromagnetic shower $Q^2 = st/u$, it is possible to keep under control, besides the large logarithms from ISR and FSR, also the leading angular contribution from initial-final state interference.

In order to estimate the precision of the PS approach with all order corrections, higher-order LL terms must be added to the exact $O(\alpha)$ cross section in the benchmark calculation. The general algorithm recently proposed in ref. [30], and there applied to the high-precision computation of the SABH cross section, can be advocated, by writing the benchmark cross section as (in the so-called additive form) [30]

$$\sigma = \sigma_{LL}^{(\infty)} - \sigma_{LL}^{(\alpha)} + \sigma_{exact}^{(\alpha)}, \quad (11)$$

where $\sigma_{LL}^{(\infty)}$ is the all-order LL cross section as given by eq. (1), $\sigma_{LL}^{(\alpha)}$ is the up to $O(\alpha)$ truncation of the LL cross section, $\sigma_{exact}^{(\alpha)}$ is the exact perturbative $O(\alpha)$ cross section of eq. (9). Collinear SFs as given in ref. [21] are used in the calculation of the LL cross sections. Adopting such a procedure, exact $O(\alpha)$ corrections are simply matched with LL higher-orders in the collinear approximation. Therefore, the cross section of eq. (11) includes exact $O(\alpha) + O(\alpha^n L^n)$, with $n \geq 2$, leading corrections.

A more accurate factorized form, as motivated and discussed in detail in ref. [30], can be supplied, by computing the cross section as

$$\sigma_F \simeq (1 + C_{NL}^{(\alpha)}) \sigma_{LL},$$

$$C_{NL}^{(\alpha)} \equiv \frac{\sigma_{exact}^{(\alpha)} - \sigma_{LL}^{(\alpha)}}{\sigma_0} \equiv \frac{\sigma_{NL}^{(\alpha)}}{\sigma_0}, \quad (12)$$

where $C_{NL}^{(\alpha)}$ is the whole NLO content of eq. (9). In such a way, the bulk of the most important second-order NLO corrections, i.e. the $O(\alpha^2 L)$ terms, are added to the content of eq. (11) [30]¹.

The procedure here shortly sketched works efficiently for cross section calculation (not unweighted event generation) and allows, by comparison with the full PS predictions, to estimate the overall precision of the PS approach. Furthermore, it is possible to get a measure of $O(\alpha^n L^n)$ and $O(\alpha^2 L)$ corrections. The benchmark calculation is available in the form of MC integrator program (LABSPV), which is a suitable modification of the SABSPV code [31] from SABH to low-energy LABH process.

5 Tests of the approach and further numerical results

As already remarked in the previous section, the detailed comparison between the exact $O(\alpha)$ cross section of eq. (9) and the up to $O(\alpha)$ expansion of the PS results is a valuable tool to establish the physical precision of the PS approach, since the registered difference is due to the NLO corrections left over in the pure LL predictions of the PS scheme. The relative difference between eq. (9) and the up to $O(\alpha)$ PS cross section is shown in Fig. 8 for the angular acceptances $20^\circ \leq \vartheta_\pm \leq 160^\circ$ and $50^\circ \leq \vartheta_\pm \leq 130^\circ$ and for two different choices of the Q^2 scale in the PS, i.e. for $Q^2 = st/u$ and $Q^2 = 0.75 \cdot st/u$. The relative deviations shown in the figure are plotted as functions of the acollinearity cut. For the “natural” choice of the scale $Q^2 = st/u$ which allows to completely reproduce the LL structure of the exact $O(\alpha)$ calculation, the difference is an unambiguous evaluation of the NLO corrections. Such contributions, as a priori expected, are important in view of the required theoretical precision, especially at the acollinearity value $\xi_{max} = 5^\circ$, being of the order of several 0.1% (see Fig. 8). However, it is worth noticing that a simple variation of the Q^2 scale from $Q^2 = st/u$ to $Q^2 = 0.75 \cdot st/u$ significantly reduces the difference, which goes from more than the 0.5-1% level down to about 0.1-0.3% at $\xi_{max} = 5^\circ$, depending on the angular set up. In general, with the adjusted scale $Q^2 = 0.75 \cdot st/u$ the difference between the exact $O(\alpha)$ calculation and the PS predictions is within 0.5%. This naive example illustrates how, for a given set of cuts, the level of agreement can be substantially improved by a simple

¹ Actually, in ref. [30] a more refined treatment of the factorized cross section is given, and it is shown that eq. (12) is an approximation of the full treatment at the 0.1% level, which is sufficient for the present study.

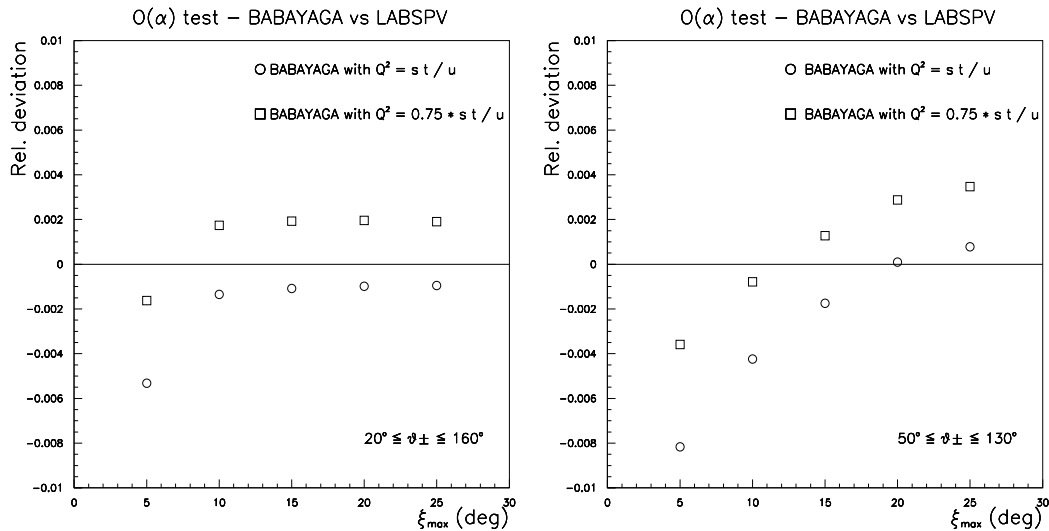


Fig. 8. Relative differences for the LABH process at the Φ factories between the exact $O(\alpha)$ cross section (LABSPV) and the up to $O(\alpha)$ PS one (BABAYAGA), as functions of the acollinearity cut and for two choices of the Q^2 scale in the electron SF. On the left the acceptance region $20^\circ \leq \vartheta_\pm \leq 160^\circ$ is considered, while on the right the acceptance region is $50^\circ \leq \vartheta_\pm \leq 130^\circ$. Other cuts are specified in the text.

redefinition of the maximum virtuality of the electromagnetic shower. Going beyond this simple procedure would require a merging between perturbative calculation and PS scheme, which is beyond the scope of the present work.

In order to assess the reliability of the PS approach in the presence of higher-order corrections, the comparison between the benchmark and PS calculation has been extended to the computation of the exact $O(\alpha)$ plus higher-orders cross section. The relative difference between eq. (11) and the full PS cross section is shown in Fig. 9, still as functions of the acollinearity cut. According to what discussed about the $O(\alpha)$ comparison, the scale in the PS is, for definiteness, fixed at $Q^2 = 0.75 \cdot st/u$. Relative differences contained within 0.5% are still observed, confirming the equivalent implementation of higher-order LL corrections in the PS and benchmark calculation. This difference between BABAYAGA and LABSPV in the presence of higher-order corrections can be considered as an estimate of the physical precision of the “modified” PS approach for the cross section calculation for realistic ES at the Φ factories.

In addition to the evaluation of the $O(\alpha)$ NLO corrections, for an assessment of the theoretical precision, it is important to evaluate the impact of the higher-order LL contributions. The size of LL $O(\alpha^n L^n)$, with $n \geq 2$, corrections can be derived, as already remarked, by comparing in the benchmark calculation the results of eq. (9) and eq. (11) or, equivalently, in the PS scheme the full all-order predictions with the corresponding up to $O(\alpha)$ truncation. Furthermore, the difference between eq. (11) and eq. (12) in the benchmark calculation is

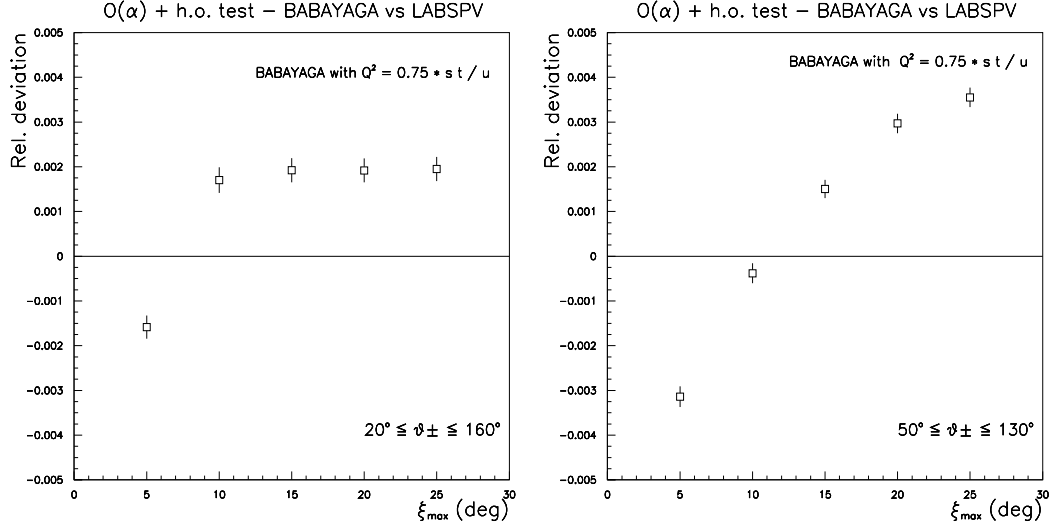


Fig. 9. The same as Fig. 8 for the $O(\alpha)$ plus higher orders Bhabha cross section at the Φ factories. Cuts are given in the text.

able to provide an indication of the size of $O(\alpha^2 L)$ corrections, thus yielding an estimate of the most important second-order NLO corrections left over in the PS method. Such an analysis of higher-order effects leads to the results shown in Fig. 10, where the relative effect of the above higher-order corrections is shown for the natural scale $Q^2 = st/u$. It can be clearly seen that LL $O(\alpha^n L^n)$ corrections are unavoidable in view of the expected theoretical accuracy. In fact, their contribution is at 1-2% level at $\xi_{max} = 5^\circ$ and of the order of some 0.1% for larger acollinearity cuts. The impact of $O(\alpha^2 L)$ is, instead, negligible, being well below the 0.1% level, in agreement with the estimate given in ref. [8].

Having established that the inclusion of higher-order contributions does not alter, as expected, the results of the $O(\alpha)$ comparison, further $O(\alpha)$ tests have been performed at the level of exclusive differential distributions. The results are illustrated in Figs. 11-13. In these plots, the histograms represent the distributions of the events generated by means of the up to $O(\alpha)$ PS generator BABAYAGA with scale $Q^2 = 0.75 \cdot st/u$, while the markers correspond to the predictions of the benchmark calculation LABSPV. A few comments are in order here. Since the benchmark calculation is not suited for unweighted event generation, the number of events corresponding to the markers have been obtained by calculating, as a first step, the integrated cross section over each bin and next by multiplying it for a reference luminosity calculated as $L = N_{PS}/\sigma_{PS}$, where N_{PS} and σ_{PS} are the number of events and the cross section obtained with the PS generator, respectively. The set of cuts used for the analysis of the distributions corresponds to the angular range 20° - 160° . Generally, as it can be seen, the level of agreement is quite satisfactory. In particular, the electron energy distribution simulated by BABAYAGA, well

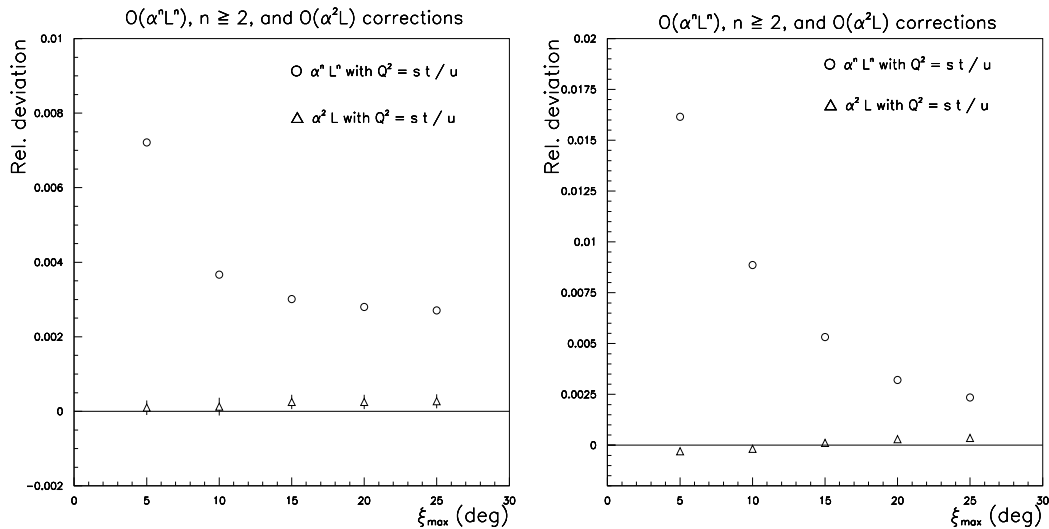


Fig. 10. Effect of higher-order $O(\alpha^n L^n)$ ($n \geq 2$) and $O(\alpha^2 L)$ corrections on the integrated Bhabha cross section at the Φ factories. On the left the acceptance region $20^\circ \leq \vartheta_{\pm} \leq 160^\circ$ is considered, while on the right the acceptance region is $50^\circ \leq \vartheta_{\pm} \leq 130^\circ$. Other cuts are specified in the text.

agrees with the exact LABSPV calculation, as shown in Fig. 11. Because the electron energy distribution is driven in the present implementation of the PS method by the x distribution of the SF, the agreement observed between exact and PS predictions reinforces, *a posteriori*, the interpretation of the x variable as residual fraction energy as the most natural one in QED PS models.

Also the PS description of the electron angular variables is in nice agreement with the exact calculation, as shown by the electron scattering angle and acollinearity distribution of Figs. 12-13. Some disagreement is seen in the first acollinearity bins, where still acceptable differences at a few per cent level are registered. The satisfactory PS predictions for the electron angles can be understood since the distributions of these variables are dominated, beyond the tree-level approximation, by the effect of the longitudinal boost due to the emission of unbalanced electron and positron ISR, which, in turn, is governed by the x distribution of the electron SF.

6 Conclusions and perspectives

The LABH process is used at present Φ and B factories as the reference reaction to determine the machine luminosity. In order to reach a total accuracy at a few 0.1% level, precision calculations of the LABH scattering cross section and distributions become more and more urgent. In particular, the relevant

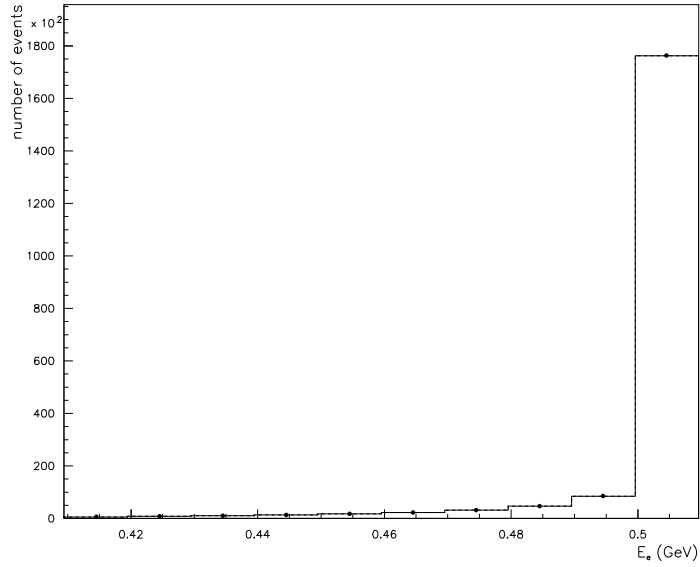


Fig. 11. Electron energy distribution for the LABH process at the Φ factories. Markers: exact $O(\alpha)$ via LABSPV. Histograms: PS prediction via BABAYAGA with scale $Q^2 = 0.75 \cdot st/u$

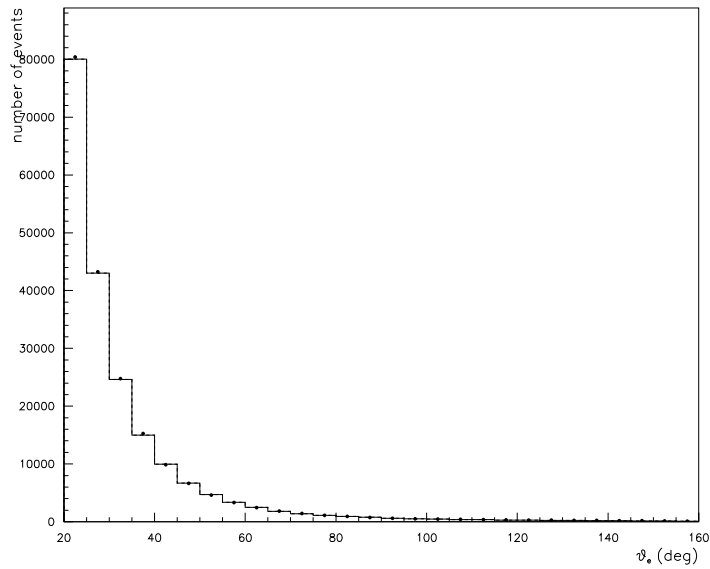


Fig. 12. Electron angle distribution for the LABH process at the Φ factories. Markers: exact $O(\alpha)$ via LABSPV. Histograms: PS prediction via BABAYAGA with scale $Q^2 = 0.75 \cdot st/u$

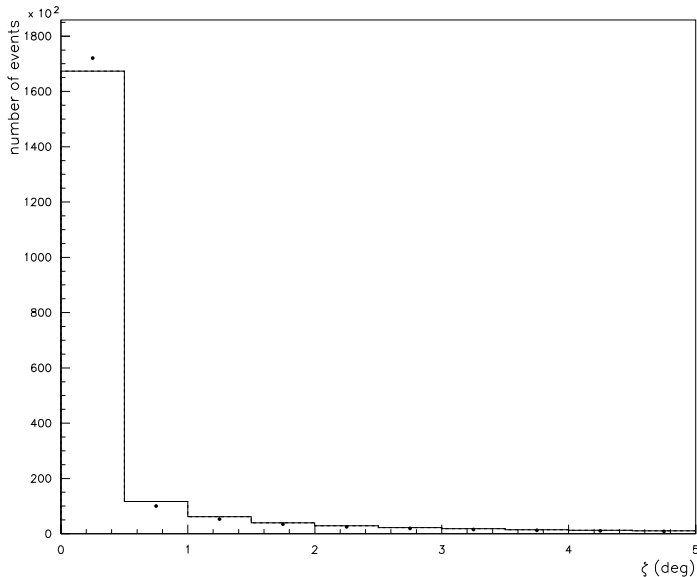


Fig. 13. Acollinearity angle distribution for the LABH process at the Φ factories. Markers: exact $O(\alpha)$ via LABSPV. Histograms: PS prediction via BABAYAGA with scale $Q^2 = 0.75 \cdot st/u$

effects due to photon emission have to be kept under control and accurately simulated in the computational tools required by the experimental analysis.

Along this direction, an original calculation of the LABH process has been addressed. It is based on a realization of the PS method in QED to account for photonic corrections due to ISR, FSR and initial-final-state interference. The approach adopted allows the calculation of integrated cross sections as well as event generation, including reconstruction of photon p_{\perp} . A new MC event generator (BABAYAGA) has been developed and is available for a full experimental simulation of the LABH process at flavour factories. The program has been used to provide several numerical results of phenomenological interest, thus showing the potential of BABAYAGA in physics analysis. For example, it has been shown, both at the level of cross section and interesting distributions, that the effects due to radiation from final-state electrons have to be carefully taken into account in the presence of realistic ES at the Φ factories DAΦNE and VEPP-2M, since the impact of FSR can be as large as the one due to ISR.

With the aim of checking the overall (physical+technical) precision of the PS approach and relative generator, a benchmark calculation has been carried out as well. It relies upon the exact $O(\alpha)$ calculation of the LABH cross section supplemented with higher-order LL corrections in the collinear approximation. The benchmark computation is also available in the form of computer code (LABSPV), which is a MC integrator allowing for precise cross section calculations, with an estimated precision at 0.1% level.

By comparing the predictions of the PS generator BABAYAGA and of the benchmark calculation LABSPV for the up to $O(\alpha)$ cross section with typical cuts, it turns out that the contribution of the $O(\alpha)$ NLO corrections is, as expected, important in the light of the required theoretical precision, being at the 0.5-1% level for typical ES at the Φ factories. However, it has been also shown that the scale Q^2 entering in the PS LL calculation can be simply adjusted in order to agree within 0.5% with the benchmark calculation. An energy scale like $Q^2 \approx st/u$ reveals to be the best choice that effectively reabsorbs $O(\alpha)$ NLO terms into LL PS contributions. This conclusion, which holds for the integrated cross section, has been proved to be generally valid also for the most interesting differential distributions.

With the scale choice $Q^2 = st/u$, the effect of higher-order $O(\alpha^n L^n)$ LL corrections has been evaluated and found to be at the 1-2% level, while the role of $O(\alpha^2 L)$ corrections is marginal, below 0.1% accuracy. Therefore, one of the main conclusions of the present analysis is that, given the size of the radiative corrections discussed above, theoretical predictions for the LABH process at flavour factories aiming at a few 0.1% precision must include the contribution of both $O(\alpha)$ NLO terms and $O(\alpha^n L^n)$ leading logarithmic contributions. From the whole of the present analysis, it turns out that the present physical precision of BABAYAGA generator is 0.5% for typical ES at the Φ factories. If particularly stringent requirements of theoretical accuracy would be in the future necessary, the PS approach as presently implemented in BABAYAGA should be updated by means of an appropriate merging of the exact $O(\alpha)$ matrix element with the exclusive photon exponentiation realized by the PS algorithm. Some proposals addressing such an issue are already available in the literature [32], in order to obtain sensible QCD phenomenological predictions for experiments at the TEVATRON and LHC.

A second possible development of the present work concerns application of the PS scheme to other phenomenological studies of strong interest at e^+e^- flavour factories. In fact, since the PS is a very general method to compute photonic radiative corrections, the same formulation here applied to the LABH process could be employed to evaluate radiative corrections to other large-angle interesting QED processes, such as $e^+e^- \rightarrow \mu^+\mu^- (n\gamma), \gamma\gamma (n\gamma)$, and also to hadronic final states, in particular for $e^+e^- \rightarrow \text{hadrons}$ and $e^+e^- \rightarrow \text{hadrons} + \gamma$, the latter of great interest for an energy scan of the hadronic cross section below the nominal c.m. energy [33].

A further foreseen development is a phenomenological analysis of QED processes at the B factories, along the lines followed in the present study.

Such possible developments are by now under consideration.

7 Acknowledgments

The authors are very grateful to A. Bukin, G. Cabibbo, S. Eidelman, V.N. Ivanchenko, F. Jegerlehner, V.A. Khoze, G. Kukartsev, J. Lee-Franzini, G. Pancheri, M. Piccolo, I. Peruzzi, Z. Silagadze and G. Venanzoni for useful discussions, remarks and interest in their work. The authors acknowledge partial support from the EEC-TMR Program, Contract N. CT98-0169. C.M. Carloni Calame and C. Lunardini wish to thank the INFN, Sezione di Pavia, for the use of computer facilities.

References

- [1] The DAΦNE physics handbook, L. Maiani, G. Pancheri and N. Paver eds., 1992.
- [2] The second DAΦNE physics handbook, L. Maiani, G. Pancheri and N. Paver eds., 1995.
- [3] G. Pancheri, *Acta Phys. Polonica* **30** (1999) 2243.
- [4] G. Cabibbo and G. Venanzoni, “Measuring the DAΦNE luminosity with large angle Bhabha scattering”, KLOE MEMO n. 168, November 9, 1998.
- [5] F.A. Berends and R. Kleiss, *Nucl. Phys.* **B 228** (1983) 537.
- [6] E. Drago and G. Venanzoni, “A Bhabha generator for DAΦNE including radiative corrections and Φ resonance”, INFN/AE-97/48, 1997.
- [7] S. Eidelman and V.N. Ivanchenko, private communication.
- [8] A.B. Arbuzov et al., *J. High Energy Phys.* **10** (1997) 001.
- [9] A.B. Arbuzov, “LABSMC: Monte Carlo event generator for large-angle Bhabha scattering”, hep-ph/9907298.
- [10] S. Jadach, W. Płaczek and B.F.L. Ward, *Phys. Lett.* **B 390** (1997) 298.
- [11] See, for example, the home page of the BABAR Event Generator Group <http://www.slac.stanford.edu/BFR00T/www/Physics/Tools/generators/>.
- [12] J. Fujimoto et al., *Prog. Theor. Phys.* **91** (1994) 333 .
- [13] H. Anlauf et al., *Comput. Phys. Commun.* **79** (1994) 466.
- [14] S. Jadach, O. Nicosini et al., “Event Generators for Bhabha Scattering”, in *Physics at LEP2*, G. Altarelli, T. Sjöstrand and F. Zwirner eds., CERN Report **96-01**, (CERN, Geneva, 1996), Vol. 2, p. 229.
- [15] See, for example, G. Montagna, O. Nicosini and F. Piccinini, *Phys. Rev.* **D 48** (1993) 1021 and references therein.

- [16] M. Greco, G. Montagna, O. Nicosini and F. Piccinini, in ref. [2], Vol. II, p. 629.
- [17] S. Eidelman and F. Jegerlehner, *Z. Phys.* **C 67** (1995) 585 .
- [18] F. Jegerlehner, private communication and DESY-99-007, [hep-ph/9901386](#), in Proc. of the IVth International Symposium on Radiative Corrections, RADCOR98, J. Sola ed., Barcelona, Spain (1998); J.G. Körner, A.A. Pivovarov and K. Schilcher, *Eur. Phys. J* **C9** (1999) 551.
- [19] V.N. Gribov and L.N. Lipatov, *Sov. J. Nucl. Phys.* **15** (1972) 298; G. Altarelli and G. Parisi, *Nucl. Phys.* **B 126** (1977) 298; Y.L. Dokshitzer, *Sov. Phys. JETP* **46** (1977) 641.
- [20] G. Montagna, O. Nicosini and F. Piccinini, *Riv. Nuovo Cim.*, Vol. **21** (1998) 1, [hep-ph/9802302](#).
- [21] E.A. Kuraev and V.S. Fadin, *Sov. J. Nucl. Phys.* **41** (1985) 466; G. Altarelli and G. Martinelli, in *Physics at LEP*, J. Ellis and R. Peccei eds., CERN Report **86-02** (CERN, Geneva, 1986), Vol. 1, p. 47; O. Nicosini and L. Trentadue, *Phys. Lett.* **B 196** (1987) 551; *Z. Phys.* **C 39** (1988) 479; F.A. Berends, G. Burgers and W.L. van Neerven, *Nucl. Phys.* **B 297** (1988) 429; M. Skrzypek and S. Jadach, *Z. Phys.* **C 49** (1991) 577; M. Cacciari et al., *Europhys. Lett.* **17** (1992) 123, G. Montagna, O. Nicosini and F. Piccinini, *Phys. Lett.* **B 406** (1997) 243, A.B. Arbuzov, *Phys. Lett.* **B 470** (1999) 252.
- [22] R. Odorico, *Nucl. Phys.* **B 172** (1980) 157, *Phys. Lett.* **B 102** (1981) 341; P. Mazzanti and R. Odorico, *Phys. Lett.* **B 95** (1980) 133; G. Marchesini and B.R. Webber, *Nucl. Phys.* **B 238** (1984) 1; T. Sjöstrand, *Phys. Lett.* **B 310** (1985) 321; K. Kato and T. Munehisa, *Phys. Rev.* **D 39** (1989) 156; K. Kato, T. Munehisa and H. Tanaka, *Z. Phys.* **C 54** (1992) 397. A review of the PS method in QCD and relative QCD event generators can be found in: R.K. Ellis, W.J. Stirling and B.R. Webber, *QCD and Collider Physics* (Cambridge University Press, 1996).
- [23] J. Fujimoto, T. Munehisa and Y. Shimizu, *Prog. Theor. Phys.* **90** (1993) 177; Y. Kurihara, J. Fujimoto, T. Munehisa and Y. Shimizu, *Prog. Theor. Phys.* **96** (1996) 1223, *ibid.* **95** (1996) 375.
- [24] H. Anlauf et al., *Comput. Phys. Commun.* **70** (1992) 97.
- [25] V.V. Sudakov, *Sov. Phys. JETP* **3** (1956) 65.
- [26] G. Bonneau and F. Martin, *Nucl. Phys.* **B 27** (1971) 381; V.N. Baier, V.S. Fadin and V.A. Khoze, *Nucl. Phys.* **B 65** (1973) 381; F.A. Berends and R. Kleiss, *Nucl. Phys.* **B 260** (1985) 32 .
- [27] M. Caffo, E. Remiddi et al., “Bhabha Scattering”, in *Z Physics at LEP1*, G. Altarelli, R. Kleiss and C. Verzegnassi eds., CERN Report **89-08** (CERN, Geneva, 1989), Vol. 1, p.171; M. Greco, *Riv. Nuovo Cim.* Vol. **11** (1988) 1.
- [28] F.A. Berends et al., *Nucl. Phys.* **B 202** (1981) 63 .
- [29] M. Greco and O. Nicosini, *Phys. Lett.* **B 240** (1990) 219.

- [30] G. Montagna, O. Nicrosini and F. Piccinini, Phys. Lett. **B 385** (1996) 348.
- [31] M. Cacciari, G. Montagna, O. Nicrosini and F. Piccinini, in Report of the Working Group on Precision Calculations for the Z Resonance, D. Bardin, W. Hollik, G. Passarino eds., CERN Report **95-03** (CERN, Geneva, 1995), p. 389, Comput. Phys. Commun. **90** (1995) 301 .
- [32] F. Krauss, R. Kuhn and G. Soff, Acta Phys. Polonica **30** (1999) 3875; G. Miu and T. Sjöstrand, Phys. Lett. **B449** (1999) 313; G. Corcella and M. Seymour, Phys. Lett. **B 442** (1998) 417; J. André and T. Sjöstrand, Phys. Rev. **D 57** (1998) 5767; H. Baer and M.H. Reno, Phys. Rev. **D 44** (1991) 3375; M.H. Seymour, Comput. Phys. Commun. **90** (1991) 95.
- [33] S. Spagnolo, Eur. Phys. J. **C6** (1999) 637; S. Binner, J.H. Kuhn and K. Melnikov, Phys. Lett. **B459** (1999) 279; M. Benayoun et al., Mod. Phys. Lett. **A14** (1999) 2605; A.B. Arbuzov et al., J. High Energy Phys. **12** (1998) 009.